

Perturbative Transport from Sawtooth Propagation and ECRH Modulation in ASDEX Upgrade

F. Ryter, M. Alexander, W. Suttrop, J. Köllermeyer, F. Leuterer, A.G. Peeters, G. Pereverzev and the ECRH, ASDEX Upgrade and NI Teams

Max-Planck-Institut für Plasmaphysik, EURATOM Association, D-85748 Garching

The comparison of transport coefficients obtained from power balance analyses and from perturbative experiments is expected to improve the understanding of transport physics [1]. This paper reports on the studies of the electron heat conductivity (χ_e) using sawtooth propagation (χ_e^{ST}) and ECRH modulation (χ_e^{ECRH}) heat pulse propagation in ASDEX Upgrade.

1. Experimental conditions

The key diagnostic in this work is the ECE radiometer which provides T_e measurements with the necessary high time resolution (31 kHz) and sensitivity (0.1 eV). This diagnostic has 45 channels generally covering 80% of the plasma minor radius ($a \approx 0.5$ m) with a radial resolution below 1 cm for each channel. The other experimental data necessary for the analyses are provided by the standard diagnostics usually available on a modern tokamak.

The recently installed first phase of the ECRH system for ASDEX Upgrade consists of one gyrotron at 140 GHz (central deposition at the second harmonic for $B_T = 2.5$ T) which delivers up to 400 kW for 0.5 s and can be modulated up to 30 kHz [2]. The modulation experiments were generally performed with 100% on/off power modulation with a duty-cycle of 50% at frequencies between 10 Hz and 1 kHz. The system allows on-axis and off-axis deposition depending on the magnetic field (B_T) and angle of injection, adjustable with a mirror.

The sawtooth and ECRH modulation studies were performed in Ohmic and NBI heated L-mode plasmas, in the standard single-null divertor configuration of ASDEX Upgrade. Plasma current, magnetic field and density as well as working gas (H^+ or D^+) were varied. All the discharges were sawtoothing which provides a wide set of data for the sawtooth analysis and a direct comparison between χ_e^{ECRH} and χ_e^{ST} in the shots where ECRH modulation was applied. We generally performed the ECRH modulation with off-axis deposition at $r/a \approx 0.5$ because this configuration offers the best conditions for χ_e analyses in the confinement region.

2. Analysis methods

Two methods were applied to analyse the data: i) a time-dependent code (TDC); ii) a Fourier transform interpreted with a slab model (FT). In the TDC analysis the diffusion equation is solved in cylindrical geometry using a forced boundary method in which the T_e time trace of one ECE channel is taken as the corresponding inner boundary condition [3]. The damping terms (electron-ion exchange, modulation of P_{OH} , radiation) are explicitly calculated. The density perturbation is generally small and not taken into account because of the lack of precise measurement. This code was recently extended with a maximum entropy fit procedure to determine χ_e [4]. TDC was essentially used for the sawtooth analysis because of the large amplitude they provide. A representative example is depicted in Fig. 1 which shows a comparison between the experimental temperature evolution at different radii and the corresponding simulation. A good agreement of the calculated time evolution of T_e with the data for $r/a \leq 0.7$ is generally obtained with flat χ_e profiles, however with larger value than χ_e^{PB} from power balance, as discussed in sect. 3.

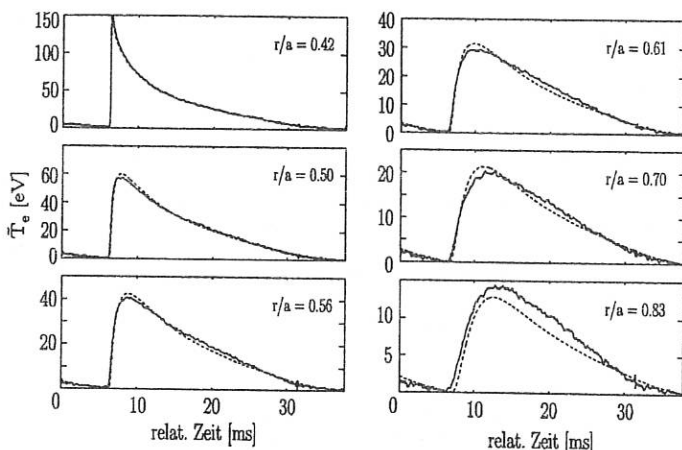


Figure 1: Fit of a sawtooth with TDC, with $\chi_e^{sim} = 4.8 \text{ m}^2/\text{s}$. The time evolution versus relative time is shown. The solid lines are the experimental time trace, the dashed lines the fit. To correctly reproduce the channels with $r/a \geq 0.7$ an outward convection of the form $U = 80(r/a)^4 \text{ m/s}$ was necessary.

An outward convection at the plasma edge is necessary to reproduce the only weakly decreasing amplitude and the flattening phase of the perturbation for $r/a \geq 0.7$. This behaviour is not modified by taking as outer boundary condition $\bar{T}_e(a) = 0$ or $\bar{T}_e(a)$ provided by the corresponding T_e measurement.

The FT analysis is less time consuming than TDC and therefore better suited for an overview of large datasets. We have verified that the TDC and FT methods give the same χ_e results within the error bars which are around $\pm 1 \text{ m}^2/\text{s}$ for both methods. The FT analysis is illustrated in Fig. 2 for an ECRH modulation dataset. It is well-known that in the slab model interpretation the amplitude and phase data for a given frequency yield χ_e^{amp} and χ_e^{phase} respectively [1]. The difference between these two values depends on the damping term, which is eliminated by taking the geometric mean, $\chi_e^{FT} = \sqrt{\chi_e^{amp} \chi_e^{phase}}$, which gives the actual χ_e^{FT} used here. It is clearly seen in Fig. 2, that the amplitude decay on the LFS and HFS of the deposition, outwards and inwards respectively, is not symmetrical. This is essentially due to the geometry effect, and it can be shown, following reference [5], that the mean value of the χ_e^{amp} values on both sides should be taken. This correction was done in this work. Note that the phase is not affected by geometry and is therefore symmetrical. It is expected that χ_e^{amp} and χ_e^{phase} reach the same value χ_e^{FT} at high frequency where the relative influence of the damping becomes weak. This behaviour is clearly observed in our experiments. For the modulation scheme used here with 50% duty-cycle, the Fourier frequency spectrum of the T_e measurement essentially shows the odd harmonics and no or very small even harmonics, as expected in the absence of non-linear reaction of the plasma to the power modulation. We also observed that, both for sawteeth and ECRH modulation, χ_e does not depend on the frequency, which excludes a T_e dependence of χ_e [6].

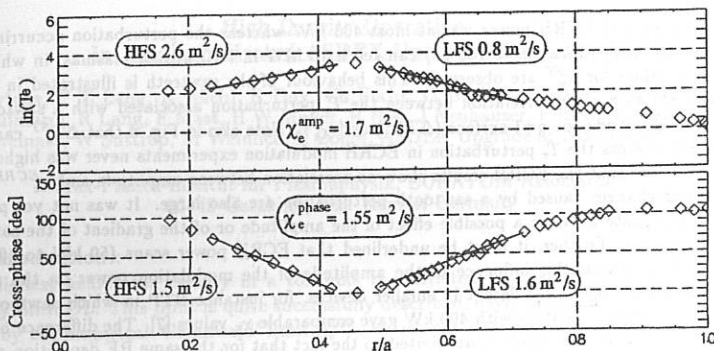


Figure 2: Example of FT results showing amplitude and cross-phase at the fundamental frequency (29.41 Hz). The linear fits for HSF and LFS are indicated as well as the mean values obtained for χ_e^{amp} , χ_e^{phase} , giving $\chi_e^{FT} = 1.6 \text{ m}^2/\text{s}$.

3. Experimental results

In this section we compare χ_e^{ST} and χ_e^{ECRH} with χ_e^{PB} , where χ_e^{PB} is given either by the power balance analysis when it is available or by $\chi_e^{Global} = a^2 \kappa / 4 \tau_E$ (κ elongation, τ_E global energy confinement time). In the cases where χ_e^{PB} was available, it has been verified that χ_e^{Global} is close to χ_e^{PB} within 25%. The analyses of our sawtooth dataset yields $\chi_e^{PB} < \chi_e^{ST} \leq 6 \chi_e^{PB}$ as appears in Fig. 3. Moreover there is obviously no correlation between χ_e^{ST} and χ_e^{PB} . In contrast, for the ECRH modulation experiments Fig. 3 clearly shows that χ_e^{ECRH} is at most 2 times larger than χ_e^{PB} , in agreement with the assumption $\chi_e \propto \nabla T_e^\alpha$ with $\alpha \leq 1$, [6].

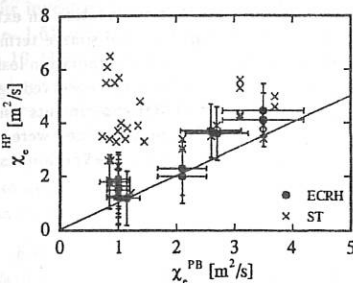


Figure 3: χ_e^{FT} or χ_e^{ECRH} versus χ_e^{PB} for Ohmic and L-mode discharges under different conditions. The χ_e^{PB} values above $2 \text{ m}^2/\text{s}$ are obtained from NBI-heated discharges in pure hydrogen.

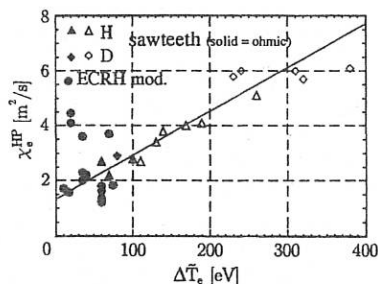


Figure 4: χ_e^{ST} plotted versus the amplitude of the temperature perturbation caused by the sawteeth as measured just outside the inversion radius.

In the shots where ECRH modulation was applied one observes that χ_e^{ST} is larger than χ_e^{ECRH} in most of the cases. An essential difference between the heat pulses from sawteeth and ECRH modulation resides in the size of the induced perturbation which is larger for sawteeth.

The modulated ECRH power was at most 400 kW whereas the perturbation occurring at a sawtooth crash (duration $\approx 100 \mu\text{s}$) can reach 10 MW in NBI heated plasmas, in which the largest values for χ_e^{ST} are observed. This behaviour of the sawteeth is illustrated in Fig. 4 which shows a clear correlation between the T_e perturbation associated with a sawtooth as measured outside the $q=1$ surface (ΔT_e^{ST}) and χ_e^{ST} . Note also in Fig. 4 that ΔT_e^{ST} can reach 400 eV whereas the T_e perturbation in ECRH modulation experiments never was higher than 60 eV. Note that the ECRH results show no correlation between amplitude and χ_e^{ECRH} . The gradient changes caused by a sawtooth perturbation are also large. It was not yet possible to discriminate between a possible effect of the amplitude or of the gradient of the sawtooth perturbation. Further, it must be underlined that ECRH power scans (50 kW to 400 kW) showed no measurable influence of the amplitude of the modulation power on the results. However, this may be different in smaller devices, for instance RTP in which sawtooth and ECRH power modulation with 400 kW gave comparable χ_e values [7]. The difference between RTP and ASDEX Upgrade is attributed to the fact that for the same RF deposition at mid-radius, the ECRH power density in RTP is larger than in ASDEX Upgrade by more than one order of magnitude due to the larger volume. A second reason might be that in ASDEX Upgrade the large discrepancies between χ_e^{ST} and χ_e^{PB} occur with auxiliary heating (up to 5 MW) where the sawteeth are the strongest. Small Ohmic sawteeth in ASDEX Upgrade yield $\chi_e^{ST} \leq 3\chi_e^{PB}$. In ASDEX Upgrade an experimental simulation of sawtooth effects with ECRH would require an installed power of several MW, which will be available in the future.

4. Discussion

Simulations of the ECRH modulation experiments described above were performed with the ASTRA code [8]. The best agreement with the data is obtained with flat χ_e profiles having values higher than that required for power balance. Similarly to the TDC results for sawteeth, for ECRH modulation also, the amplitude and phase behaviour for channels outside $r/a = 0.7$ are well reproduced with outward convection. However, the observed behaviour might also be caused by a non-local transport, which introduces into the diffusion equation an extra modulated source term linked to the steady-state source [6]. In our case, the source term is dominated by the heating power inside $r/a = 0.7$ whereas it is dominated by the radiation losses outside this radius. In particular, the latter term qualitatively reproduces the observed edge behaviour of the perturbation at the edge. The simulations of our ECRH experiments using a non-local transport model also show that even harmonics should be created. They were not experimentally observed, perhaps due to a lack of sensitivity. Therefore, in our experiments, a non-local character of transport cannot yet be fully excluded.

References

- [1] LOPES-CARDOZO, N. J., *Plasma Phys. Controlled Fusion* **37** (1995) 799.
- [2] LEUTERER, F. et al., *This Conference* (1996).
- [3] RIEDEL, K. S. et al., *Nucl. Fusion* **38** (1988) 1509.
- [4] GIANNONE, L. et al., *Plasma Phys. Controlled Fusion* **38** (1996) 477.
- [5] JACCHIA, S. et al., *Phys. Fluids B* **3** (1991) 3033.
- [6] STROTH, U. et al., *Plasma Phys. Controlled Fusion* **38** (1996) 611.
- [7] JACCHIA, S. et al., *Nucl. Fusion* **34** (1994) 1629.
- [8] PEREVERZEV, G. V. et al., IPP report 5/42 (1991).